Proceedings of the IEEE 2020 25th International Conference on Pattern Recognition (ICPR), 10-15 January, Milan, Italy
DOI:10.1109/ICPR48806.2021.9412838

DCT/IDCT Filter Design for Ultrasound Image Filtering

Barmak Honarvar Shakibaei[1,2,*], Jan Flusser[1], Yifan Zhao[2], John Ahmet Erkoyuncu[2] and Rajkumar Roy[3]

[1]Czech Academy of Sciences, Institute of Information Theory and Automation, Pod vodárenskou věží 4, 18208 Praha 8, Czech Republic
Email: {honarvar,flusser}@utia.cas.cz

[2]Through-Life Engineering Services Centre, School of Aerospace, Transport and Manufacturing, Cranfield University, Bedfordshire MK43 0AL, UK
Email: {barmak,yifan.zhao,j.a.erkoyuncu}@cranfield.ac.uk

[3]School of Mathematics, Computer Science and Engineering City, University of London, Northampton Square, London, EC1V 0HB, UK
Email: r.roy@city.ac.uk

***Abstract*—In this paper, a new recursive structure based on the convolution model of discrete cosine transform (DCT) for designing of a finite impulse response (FIR) digital filter is proposed. In our derivation, we start with the convolution model of DCT-II to use its Z-transform for the proposed filter structure perspective. Moreover, using the same algorithm, a filter base implementation of the inverse DCT (IDCT) for image reconstruction is developed. The computational time experiments of the proposed DCT/IDCT filter(s) demonstrate that the proposed filters achieve faster elapsed CPU time compared to the others. The image filtering and reconstruction performance of the proposed approach on ultrasound images are presented to validate the theoretical framework.**

I. Introduction

DCT has found wide applications in signal and image processing in general, and in data compression, filtering and feature extraction in particular. The DCT has been proved successful at decorrelating and correlating the energy of image data. After decorrelation, each DCT coefficient can be encoded independently without lossing compression efficiency since it has a strong 'energy compation' property in typical applications [1]. In comparison to discrete Fourier transform (DFT), DCT is a real transform that transforms a sequence of real data points into its real spectrum and therefore avoids the problem of redundancy. Also, as DCT is derived from DFT, all the desirable properties of DFT (such as the fast algorithm) are preserved. To reduce DCT computational complexities, the development of fast and efficient algorithms for computing 2-D DCT/IDCT becomes increasingly important. Various fast algorithms for computing 2-D DCT were proposed to minimize the computational complexity [2]. However, there are a variety of DCT of which four are common (DCT-I, DCT-II, DCT-III, and DCT-IV). Each differs by only a bit, and each has its own usage in particular field. For image reconstruction, DCT II is used to decompose and DCT III is used to reconstruct. Each DCT has its cosine basis kernel which is orthogonal. The most common variant of discrete cosine transform is the type-II DCT, which is often called simply "the DCT". Its inverse is correspondingly often called simply "the inverse DCT" or "the IDCT". The N-point DCT-II of a discrete signal, $x(n)$ is given by

$$X_k = c(k) \sum_{n=0}^{N-1} x(n) \cos\left[\frac{\pi}{N}\left(n+\frac{1}{2}\right)k\right], \qquad (1)$$

for $k = 0, 1, \ldots, N-1$, where

$$c(k) = \begin{cases} \dfrac{1}{\sqrt{N}}, & k = 0 \\ \sqrt{\dfrac{2}{N}}, & \text{otherwise.} \end{cases}$$

The above scale factor can be rewritten in terms of the unit impulse and step functions as $c(k) = \left[\delta(k) + \sqrt{2}u(k-1)\right]/\sqrt{N}$. The inverse 1-D discrete cosine transform (IDCT)-II can be defined as

$$x(n) = \sum_{k=0}^{N-1} c(k) X_k \cos\left[\frac{\pi}{N}\left(n+\frac{1}{2}\right)k\right], \qquad (2)$$

for $n = 0, 1, \ldots, N-1$.

Medical ultrasound images are usually corrupted by noise in its acquisition and transmission. Hand-held ultrasound scanners are increasingly being employed at the point of care and used in telemedicine to serve rural population limited access to hospitals [3]. However, image quality of these portable systems are in general poorer than those of standard scanners. They are also often used in scans by physicians rather than by expert sonographers. Thus, the poor image quality is one of major drawbacks of the ultrasound image due to speckle noise. In general, ultrasound images have two main noise components - electronic noise, modeled as an additive white Gaussian noise, and speckle noise. In raw RF data, speckle noise is multiplicative but in the B-mode image we consider it as an additive noise due to the log transform. Speckle noise is correlated with the signal and is not Gaussian [4]. However,

© 2021 IEEE. Personal use of this material is permitted. Permission from IEEE must be obtained for all other uses, in any current or future media, including reprinting/republishing this material for advertising or promotional purposes, creating new collective works, for resale or redistribution to servers or lists, or reuse of any copyrighted component of this work in other works.

the proposed denoising suppresses all additive components regardless of their probability distribution. On the other hand, multiplicative speckle noise is generally more difficult to remove than additive noise, because the intensity of the noise varies with the image intensity [5]. Image noise is usually random, but ultrasound speckle is not random and results from some patterns of constructive and destructive interference shown as bright and dark dots in the image. Sometimes speckle helps to identify the boundaries better in ultrasound images than without speckle. In addition to speckle, there is thermal noise in ultrasound images arising due to electronics. In this research, the proposed method deals with the additive noise which is pertinent to addressing the image quality of low cost scanners in which noise performance of amplifiers may be low compared to high end scanners. The proposed method also allows for reconstruction after compression which may be necessary in telemedicine (when images will need to be transmitted over limited band widths). The presence of speckle noise affects difficulties on features extraction and quantitative measurement of ultrasound images. There are some algorithms to suppress the speckle noise while attempting to preserve the image content using combination of Gaussian filter and DCT approach [6]. Furthermore, the main challenge in image denoising techniques is to remove such noises while preserving the important features and details. Filtering techniques can be classified as single scale spatial filtering (linear, nonlinear, adaptive methods, etc.) and multiscale filtering (anisotropic diffusion-based methods, DCT, Wiener, wavelet, curvelet, contourlet, etc.). Mean filtering and Gaussian filtering are the examples of linear methods which blur the sharp edges, destroy lines and suppress the details [7], [8]. The authors in [8] also showed that filtering efficiency depends considerably on DCT coefficient statistics.

In this paper, our approach toward deriving an FIR filter structure is based on a convolution equation to simplify 1-D DCT in terms of the flipped input signal. We then obtain the transfer function of the FIR filter in Z-domain to find a simple filter structure of DCT coefficients generation [9], [10]. Finally, using the orthogonality property of cosine function, we derive the IDCT-II FIR filter structure to recover the original signal based on its limited DCT-II coefficients by applying the same method of transfer function design. The main contribution of this study is in developing a new computational algorithm for denoising of ultrasound images to have a better image quality performance. Moreover, the proposed FIR filters make an automatic system to accelerate the generated DCT coefficients to apply it for the proposed DCT-based ultrasound image filtering.

II. Derivation of a Recursive Algorithm for 1-D DCT and IDCT

Before deriving a recursive algorithm for 1-D DCT based on FIR digital filter structure, we show how to get a 1-D signal transform based on any kernel function using a simple discrete convolution in the following Theorem.

Theorem 1. A discrete transformation of a discrete signal, $f(n)$ of length N, over a kernel function of $g(n,k)$ can be derived by the discrete convolution of the kernel and the flipped signal which is evaluated at $N-1$.

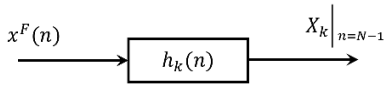

Fig. 1: A simple FIR filter structure with impulse response $h_k(n)$ for generating DCT-II coefficients from a flipped input signal.

Proof. The discrete transform for a 1-D signal $f(n)$ of length N with any kernel function of $g(n,k)$, can be written as:

$$F_k = \sum_{n=0}^{N-1} f(n)g(n,k). \tag{3}$$

By changing n to $N-1-n$, the above equation can be written as:

$$\begin{aligned} F_k &= \sum_{n=0}^{N-1} f(N-1-n)g(N-1-n,k) \\ &= \sum_{n=0}^{N-1} f^F(n)g(N-1-n,k) \\ &= f^F(n) * g(n,k)\Big|_{n=N-1}, \end{aligned} \tag{4}$$

where $f^F(n)$ is the flipped version of the input signal. Using the definition of 1-D discrete convolution for the above equation, we end up with $\sum_{n=0}^{N-1} f(n)g(n,k) = f^F(n) * g(n,k)\Big|_{n=N-1}$, which completes the proof of Theorem 1. □

A. FIR filter implementation for 1-D DCT-II

By applying Theorem 1 to DCT-II definition in (1) and considering the kernel function as a cosine signal, $g(n,k) = \cos\left[\frac{\pi}{N}\left(n+\frac{1}{2}\right)k\right]$, we get:

$$\begin{aligned} X_k &= c(k)\sum_{n=0}^{N-1} x(n)\cos\left[\frac{\pi}{N}\left(n+\frac{1}{2}\right)k\right] \\ &= c(k)\left\{x^F(n) * h_k(n)\Big|_{n=N-1}\right\}, \end{aligned} \tag{5}$$

where $h_k(n) = \cos\left[\frac{\pi}{N}\left(n+\frac{1}{2}\right)k\right]$. The function $h_k(n)$ is called the digital filter impulse response which is the same as kernel function $g(n,k)$. Such a system is shown in Fig. 1. The system feeds by a flipped signal and generates the DCT-II coefficients which are sampled at $N-1$.

To find the FIR filter structure of the above system, it is easy to obtain the transfer function of the system in Z-domain ($H_k(z)$). We start to expand the cosine function of $h_k(n)$ as follow:

$$h_k(n) = \alpha_k \cos\left(\frac{\pi nk}{N}\right) - \beta_k \sin\left(\frac{\pi nk}{N}\right), \tag{6}$$

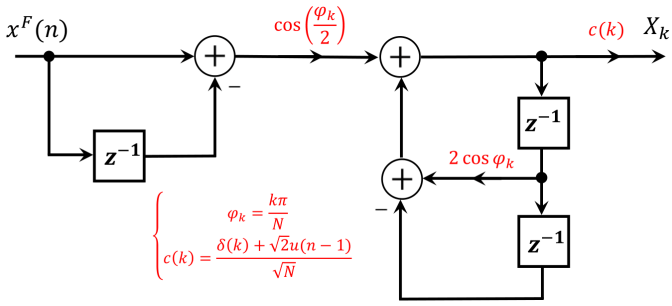

Fig. 2: DCT network: Recursive FIR filter structure to generate DCT-II coefficients for $k = 0, 1, \ldots, N-1$.

where $\alpha_k = \cos\left(\frac{\pi k}{2N}\right)$ and $\beta_k = \sin\left(\frac{\pi k}{2N}\right)$.

By taking the Z-transform of (6), we can find the transfer function of the FIR filter as:

$$H_k(z) = \frac{z\left[z - \cos\left(\frac{\pi k}{N}\right)\right]\alpha_k - z\sin\left(\frac{\pi k}{N}\right)\beta_k}{z^2 - 2z\cos\left(\frac{\pi k}{N}\right) + 1}. \tag{7}$$

Let $\varphi_k = \frac{\pi k}{N}$, then $\alpha_k = \cos\left(\frac{\varphi_k}{2}\right)$ and $\beta_k = \sin\left(\frac{\varphi_k}{2}\right)$. Eq. (7) can be rewritten as:

$$H_k(z) = \frac{\alpha_k - (\alpha_k\cos\varphi_k + \beta_k\sin\varphi_k)\,z^{-1}}{1 - 2z^{-1}\cos\varphi_k + z^{-2}}. \tag{8}$$

On the other hand, $\alpha_k\cos\varphi_k + \beta_k\sin\varphi_k = \alpha_k$, then Eq. (8) can be simplified as:

$$H_k(z) = \frac{\alpha_k\left(1 - z^{-1}\right)}{1 - 2z^{-1}\cos\varphi_k + z^{-2}}. \tag{9}$$

The transfer function in Eq. (9) can be implemented as an FIR filter in Fig. 2. This filter contains three delay units and three adders. Moreover, the filter uses three multipliers and two negative feedback. The outputs of filter are sampled at $N-1$ to generate DCT coefficients for each different values of k. The FIR system is quite simple since we have used the flipped version of the original signal as system input unlike the existing algorithms [2].

B. FIR filter implementation for 1-D IDCT-II

For IDCT-II which is described in (2), it is possible to apply the same theorem and consider the same kernel function with respect to k as the independent variable to get the following convolution:

$$\begin{aligned} x(n) &= \sum_{n=0}^{N-1} c(k)X_k\cos\left[\frac{\pi}{N}\left(n+\frac{1}{2}\right)k\right] \\ &= Y^F(k) * h_n(k)\Big|_{k=N-1}, \end{aligned} \tag{10}$$

where $h_n(k) = \cos\left[\frac{\pi}{N}\left(n+\frac{1}{2}\right)k\right]$ and $Y(k) = c(k)X_k$. Note that here, the impulse response $h_n(k)$ is different with the earlier impulse response $h_k(n)$ because of the concept of the independent variable in signals theory. Taking the Z-transform of $h_k(n)$ with respect to the independent variable k and using

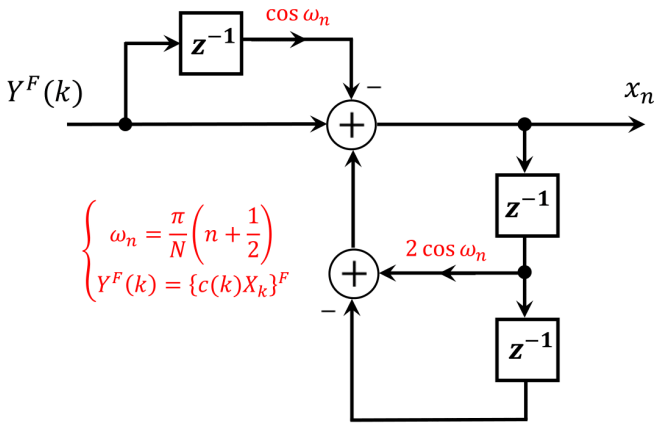

Fig. 3: IDCT network: Recursive FIR filter structure to reconstruct the original signal from its DCT-II coefficients for $n = 0, 1, \ldots, N-1$.

the Z-transform of the cosine function, the FIR filter transfer function can be written as:

$$H_n(z) = \frac{1 - z^{-1}\cos\omega_n}{1 - 2z^{-1}\cos\omega_n + z^{-2}}, \tag{11}$$

where $\omega_n = \frac{\pi}{N}\left(n+\frac{1}{2}\right)$. The transfer function in (11) can be implemented as an FIR filter which is shown in Fig. 3. This filter also contains three delay units and two adders as well as two multipliers and two negative feedback. The outputs of filter are sampled at $N-1$ to recover the original signal for each different values of n. The structure also has the flipped version of the DCT coefficients which is multiplied by the scale factor $c(k)$.

C. Recursive Formulas for DCT and IDCT Based on the Proposed Algorithms

The obtained transfer functions in (9) and (11) are in the form of $Y_{out}(z)/X_{in}(z)$. Therefore, by knowing that each delay term in Z-domain such as $z^{-m}Q(z)$, provides a difference form of $q(n-m)$ for all integer m and assumed signal, $q(n)$, we can find a difference relation of the aforementioned equations which are the same as a recurrence formula of the system. For the first transfer function in (9) which is shown as an FIR filter in Fig. 2, we have the following recurrence relation:

$$\begin{aligned} X_k(n) = c(k)\Big\{&\left[x^F(n) - x^F(n-1)\right]\cos\left(\frac{\varphi_k}{2}\right) \\ &+ 2\cos\varphi_k X_k(n-1) - X_k(n-2)\Big\}, \end{aligned} \tag{12}$$

where $k = 0, 1, \ldots, N-1$ and $X_k(-1) = X_k(-2) = 0$. The second transfer function in (11) that is shown in Fig. 3, can be converted to a recursive formula for reconstructing the original signal as:

$$\begin{aligned} x_n(k) = Y^F(k) - (\cos\omega_n)\,Y^F(k-1) + 2\cos\omega_n \\ \times x_n(k-1) - x_n(k-2), \end{aligned} \tag{13}$$

where $n = 0, 1, \ldots, N-1$ and $x_n(-1) = x_n(-2) = 0$. Equation (12) uses n as the independent variable while Eq. (13) presents k as the independent variable for our derived recursive formulas.

III. Generalized Algorithms for 2-D DCT/IDCT Implementation

The same implementation could be applied for 2-D DCT-II since there is a kernel separation for it and the transfer function of 2-D FIR filter can be obtained from multiplication of two transfer functions described in (9) and (11). The implementation of 2-D FIR filter could be also generalized using the 2-D convolution version of (5). The same procedure can be applied for 2-D version of (10) to find the proper FIR filter design for 2-D IDCT. For recursive formulas of 2-D DCT, we can follow 2-D version of (9) to obtain the following recurrence relation for computing 2-D DCT:

$$\begin{aligned} X_{k_1,k_2}(n,m) = c_1(k_1)c_2(k_2)\Big\{ & \Big[x^F(n,m) - x^F(n-1,m) \\ & - x^F(n,m-1) + x^F(n-1,m-1)\Big] \\ & \times \cos\left(\frac{\varphi_{k_1}}{2}\right)\cos\left(\frac{\varphi_{k_2}}{2}\right) \\ & + 2\cos\varphi_{k_1}\Big[X_{k_1,k_2}(n-1,m) \\ & + X_{k_1,k_2}(n-1,m-2)\Big] \\ & + 2\cos\varphi_{k_2}\Big[X_{k_1,k_2}(n,m-1) \\ & + X_{k_1,k_2}(n-2,m-1)\Big] \\ & - 4\cos\varphi_{k_1}\cos\varphi_{k_2}X_{k_1,k_2}(n-1,m-1) \\ & - X_{k_1,k_2}(n,m-2) - X_{k_1,k_2}(n-2,m) \\ & - X_{k_1,k_2}(n-2,m-2)\Big\}, \end{aligned} \tag{14}$$

for $k_1, n = 0, 1, \ldots, N-1$ and $k_2, m = 0, 1, \ldots, M-1$ where $c_1(k_1) = \left[\delta(k_1) + \sqrt{2}u(k_1-1)\right]/\sqrt{N}$, $c_2(k_2) = \left[\delta(k_2) + \sqrt{2}u(k_2-1)\right]/\sqrt{M}$, $\varphi_{k_1} = \pi k_1/N$ and $\varphi_{k_2} = \pi k_2/M$ (for an image with size of $N \times M$). It is easy to find a similar recursive formula as above for reconstructing the original image via its 2-D IDCT coefficients.

IV. Experimental Results

The simulations have been performed using a wide set of captured images based on different fetal scans (normal and anomaly). These scans were performed in a trajectory (axially from head to toe or toe to head followed by sagittally in the opposite direction) in a display-less mode. All images were extracted from different sets of videos. We selected normal fetus, fetal cystic hygroma and fetal hydronephrosis from the fetus ultrasound images for our experiments. Fig. 4 shows some of the fetus ultrasound images that we used for our experiments. Note that the aim of the experiments is to show that the proposed recursive algorithm for DCT computation can be efficiently used as a plug-in into denoising and reconstruction algorithms. We illustrate this on medical ultrasound data.

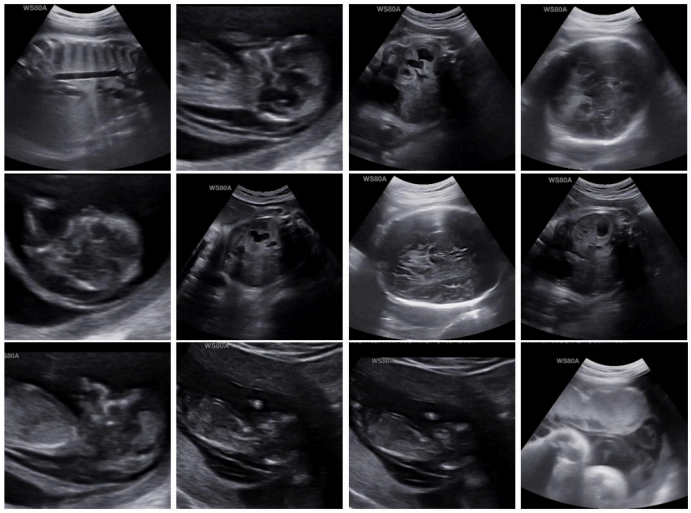

Fig. 4: Some examples of fetus ultrasound data-set images used for experiments. The size of all images is 400×400.

A. Computational Time

In DCT calculation, the time is a critical issue because in general the calculation of DCT coefficients is time expensive and fast algorithms may help a lot. Their importance is even more apparent if we are aware that a typical application of DCT is in image compression where a close-to-real time performance is desirable. We tested the time complexity of the proposed methods and compared it to two reference algorithms: the direct recursive structure method [2] and the fast discrete cosine transform (FDCT) algorithm that utilizes the energy compactness and matrix sparseness properties in frequency domain to achieve higher computation performance [11]. The computational complexity of the proposed recursive structures is compared with those of the existing ones [2], [11]. For the fast algorithms of the 2-D DCT, the recursive structures for computing radix-r technique is applied in [2] and the number of additions is reduced to at least 30% of method [12]. The number of multiplications has no reduction and is increased more than 100% which is a drawback of this method. For the second fast DCT method described in [11], the authors achieved a 40% of reduction in the number of multiplications with no improvement for decreasing of the additions number. To compare those algorithms with the proposed method using digital filter technique, we obtained a 71% and 34% decrement in the number of multiplications comparing to [2] and [11], respectively. In terms of the number of additions, the proposed method has almost a 79% reduction in comparison with [2]. Table I shows a comparison of the number of multiplications and additions for computation of DCT coefficients based on three different fast algorithms applied to all test images (size of 400×400) which are presented in Fig. 4. Since the proposed algorithm is developed based on the DCT filter structure, there are many reductions in the number of additions and multiplications. The advantage of the proposed technique is in

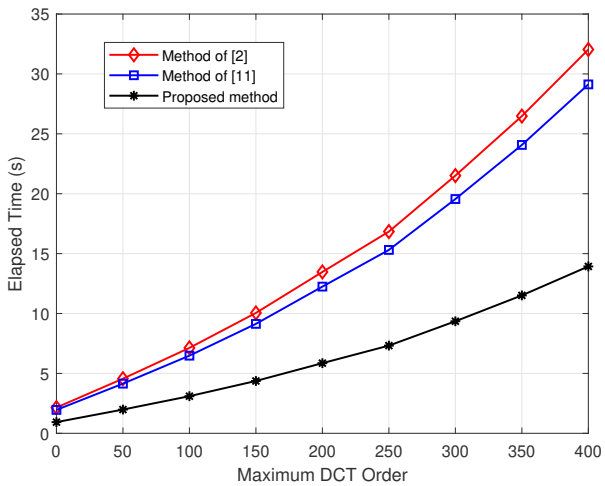

Fig. 5: Average elapsed CPU times in seconds: full set of DCT coefficients extraction for ultrasound data-sets using different methods.

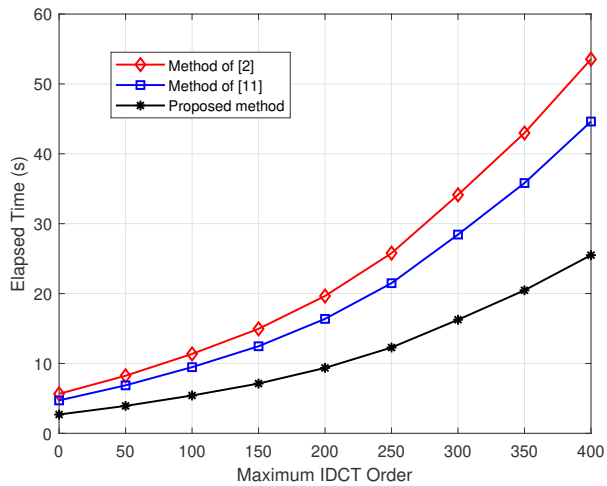

Fig. 6: Average elapsed CPU times in seconds: full set of IDCT image reconstruction for ultrasound data-sets using different methods.

decreasing the number of additions while in [2] by decreasing the number of multiplications, the number of additions starts to increase which is a big drawback of the existing algorithms.

As can be seen from Fig. 5, the average elapsed time for calculation the full DCT coefficients of our test ultrasound images using proposed method is much better than [2] and [11]. One of the most important advantage of the proposed method is eliminating the pre-addition blocks of the existing algorithms. We run the same speed test for the average elapsed time of computing original image using its DCT coefficients through IDCT filter structure. Fig. 6 clearly shows that the speed performance of the IDCT recursive method for image reconstruction from a set of finite DCT coefficients is significantly faster than the other mentioned methods.

B. DCT-based Ultrasound Image Filtering

The state-of-the-art filters including the DCT-based denoising [8], [13] and the Wiener-based techniques [14] provide filtering performances for complex structure images and large noise variance. In this paper, we use the Wiener DCT-based image filtering with hard threshold. As discussed earlier, the speckle noise of medical ultrasound image is modeled as multiplicative noise and non-Gaussian distributed [15] and defined by:

$$g(n,m) = x(n,m)v(n,m) + \eta(n,m), \tag{15}$$

TABLE I: Number of multiplication and addition operations for computation of DCT coefficients based on three different methods for all fetus ultrasound test images shown in Fig. 4 with size 400×400.

Operation	Fast algorithms		Proposed algorithm
	[2]	[11]	
Multiplication	560	245	**162**
Addition	2450	N/A	**520**

where $g(n,m)$ is an observed noisy image, n and m are the image pixel values, $x(n,m)$ denotes a noise-free image, $v(n,m)$ and $\eta(n,m)$ are multiplicative noise and white Gaussian noise not correlated with $x(n,m)$, respectively. It is suggested that the additive noise has weaker effect than the multiplicative noise of medical ultrasound image. Consequently, (15) can be written as:

$$g(n,m) \approx x(n,m)v(n,m). \tag{16}$$

Laplace and Rayleigh distribution have been used to model the multiplicative noise distribution. For the B-Scan ultrasound images, the logarithmic compression is applied and then (16) is rewritten as:

$$\log g(n,m) \approx \log x(n,m) + \log v(n,m). \tag{17}$$

Then, the multiplicative noise becomes the additive noise and is approximated as an additive zero mean Gaussian noise [15]. It means, we could consider $g(n,m) \approx x(n,m) + v(n,m)$ as the new model of ultrasound images in our coming experiments in logarithmic mode. Similar to Wiener filter, the target is to find an estimate of the noise-free image $\widehat{x}(n,m)$ such that it minimizes the mean square error (MSE). Thus, the Wiener DCT-based filter in the DCT domain can be formulated as:

$$\widehat{H}_W(k_1,k_2) = \frac{\widehat{P}_x(k_1,k_2)}{\widehat{P}_x(k_1,k_2) + \lambda(k_1,k_2)\sigma^2}, \tag{18}$$

where $\widehat{H}_W(k_1,k_2)$ is an estimate of the frequency response of the Wiener filter and $\widehat{P}_x(k_1,k_2)$ is power spectral density estimates of the noise-free image and σ^2 is noise variance since $\lambda(k_1,k_2)$ is proportional to the image size, and $\lambda(0,0) = 0$ because we assume the Gaussian noise to have zero mean.

We use the DCT instead of the Fourier transform for spectrum calculation in standard Wiener filter, i.e., $\widehat{P}_x(k_1,k_2) = X^2_{k_1,k_2}$, where X_{k_1,k_2} is the DCT of a noise-free image.

In practice the noise-free image is not accessible to obtain X_{k_1,k_2}. For this reason, the estimate of image power spectral density, $\widehat{P}_x(k_1,k_2)$, should be calculated using an observed noisy image. Therefore, the image data has to be pre-filtered to obtain some rough estimate of a noise-free image $\widehat{X}_{k_1,k_2}$ and then to calculate $\widehat{P}_x(k_1,k_2)$ to implement the Wiener filter in (18).

The last expression for the Wiener DCT-based filter transfer function, Eq. (18), could be simplified assigning the unit gain for all spatial DCT coefficients where $|U(k_1,k_2)| \geq \beta\sigma$ and zero gain otherwise. This results in a hard thresholding technique:

$$H_T(k_1,k_2) = \begin{cases} 1 & ; \quad |U(k_1,k_2)| \geq \beta\sigma \\ 0 & ; \quad \text{otherwise} \end{cases} \quad , \qquad (19)$$

where β is a control parameter. For our second experiment which is denoising of ultrasound images based on the proposed DCT filter structure, β can be varied from 0 to 1 based on its quasi-optimal value [16]. Fig. 7 illustrates DCT filtering efficiency for three sets of data: first row is the normal fetus, second row is the fetal cystis hygroma and the third row shows the fetal hydronephrosis. The sizes of all images are 400×400 pixels. Each image was denoised using a DCT-based Wiener filter led by the proposed FIR filter structure with different level of thresholds ($\beta = 0.1, 0.5, 0.8$). To show the quality of filtered images, we use the statistical-normalization image reconstruction error (SNIRE) in [17] to measure the difference between the original image and the enhanced image by using pixel values. Moreover, the blind/referenceless image spatial quality evaluator (BRISQUE) is applied to get a score for image measurement from a natural image model [18]–[20]. For this score, lower values conduct us to a better subjective quality. These scores show that the quality of enhanced images are improved after DCT filtering processes. Furthermore, we compare the proposed algorithm with classical image denoising method followed by conventional Wiener filter. The last column in Fig. 7 shows the results for the denoised image of the original image illustrated in the first column of the figure by using Wiener filter. The second, third and forth columns show the proposed DCT-based method to denoise the original images with different level of hard thresholds. It can be seen from the forth and last columns of the figure, when $\beta = 0.1$ the proposed algorithm has better performance and quite good improvements than the classical Wiener filter method. Both SNIRE and BRISQUE criterion confirm the effectiveness of the proposed algorithm.

C. Ultrasound Image Reconstruction Using Proposed Filter Structure

To show different reconstruction and recognition abilities of the proposed IDCT filter, we carried out the following experiment. Fig.8 shows the same ultrasound images that we used for the previous experiment for denoising algorithms. We calculated DCT coefficients using the recursive proposed method up to order 400 which should theoretically provide a possibility of loss-less reconstruction. We reconstructed the original image using various DCT coefficients orders (maximum reconstruction orders are 50, 100, 200, 300 and 400 for all images). We used the SNIRE and the structural similarity (SSIM) index to measure the performance of the proposed IDCT filtering. Lower values of SNIRE and higher values of SSIM means a better reconstruction with less error. The obtained results for both SNIRE and SSIM in Fig.8 illustrate a better image reconstruction. For example, in the first row of this figure, reconstruction using IDCT filter provides 77% improvement with order of 300 in comparison with 50.

Fig. 9 shows the image reconstruction error analysis with increasing rate of the DCT orders. This figure also illustrates that an optimal trade-off between the accuracy and complexity is provided by the maximum DCT order between 50 and 100, depending on the data.

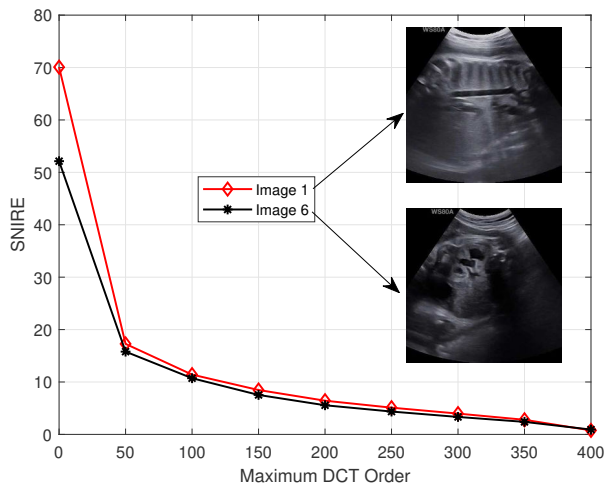

Fig. 9: Image reconstruction error analysis by increasing DCT orders. In the legend of graph, Images 1 and 6 refer to the original images in the first and sixth rows of Fig. 7.

V. Conclusion

In this paper, a new approach has been proposed for DCT/IDCT calculation based on FIR filter structures and presented its performance on ultrasound image filtering and reconstruction. This approach has been developed using convolution model of DCT to use its Z-transform for designing an FIR digital filter network. The same approach has been used to find a recursive filter to reconstruct ultrasound images using IDCT structure. In order to evaluate the performance of the new filters, a set of normal/abnormal fetus ultrasound images have been applied to test the validity of the proposed algorithms. It has also been shown that filtering efficiency depends considerably on hard thresholding. By choosing a correct threshold level, the denoising results using our method is better than the classical Wiener filter denoising while the proposed filter is simpler and faster. Additionally, to illustrate the proposed method accuracy, BRISQUE, SNIRE and SSIM indexes showed the image quality scores, the error measurement and the structural similarity in our analysis, respectively.

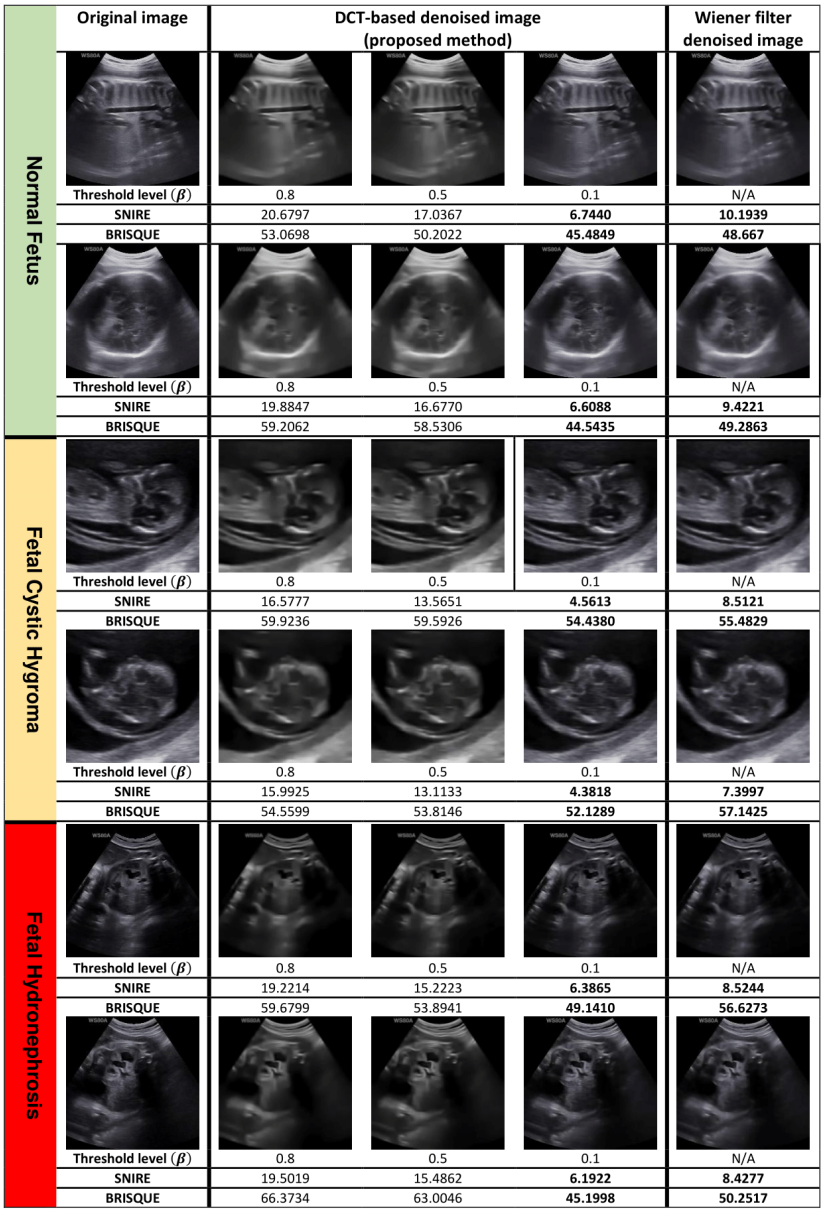

Fig. 7: DCT Filtering results for the real fetal ultrasound images captured for normal/anomaly fetuses using DCT-based proposed method compared to classical Wiener filtering. The last two columns show that the proposed method is performing denoised process better than Wiener filter.

The main advantage of our method is the speed and the ability to perform both lossy and loss-less reconstruction.

Acknowledgment

This work has been supported by the Czech Science Foundation (Barmak Honarvar with Grant No. 18-26018Y and Jan Flusser with Grant No. GA18-07247S). It has also been supported by the UK EPSRC GCRF Grant: Distributed Intelligent Ultrasound Imaging System for Secure in-community Diagnostics (SecureUltrasound) (Grant number EP/R013950/1).

References

[1] N. Ahmed, T. Natarajan, and K. R. Rao, "Discrete cosine transform," *IEEE Transactions on Computers*, vol. C-23, no. 1, pp. 90–93, Jan 1974.

[2] Che-Hong Chen, Bin-Da Liu, and Jar-Ferr Yang, "Direct recursive structures for computing radix-r two-dimensional DCT/IDCT/DST/IDST," *IEEE Transactions on Circuits and Systems I: Regular Papers*, vol. 51, no. 10, pp. 2017–2030, Oct 2004.

[3] J. Wright, O. Noriega, and H. Ho, "The application of hand-held ultrasound scanner in teaching of telemedicine and rural medicine," *Donald Sch J Ultrasound in Obstet Gynecol*, vol. 8, pp. 87–91, 2014.

[4] P. Coupé, P. Hellier, C. Kervrann, and C. Barillot, "Nonlocal means-based speckle filtering for ultrasound images," *IEEE transactions on image processing*, vol. 18, no. 10, pp. 2221–2229, 2009.

[5] P. Hiremath, P. T. Akkasaligar, and S. Badiger, "Speckle noise reduction in medical ultrasound images," in *Advancements and Breakthroughs in Ultrasound Imaging*, G. Gunarathne, Ed. IntechOpen, 2013, ch. 8.

[6] S. Riyadi, M. M. Mustafa, A. Hussain, O. Maskon, and I. F. M. Noh, "Quasi-gaussian dct filter for speckle reduction of ultrasound images," in *Visual Informatics: Bridging Research and Practice*, H. Badioze Zaman, P. Robinson, M. Petrou, P. Olivier, H. Schröder, and T. K. Shih, Eds. Berlin, Heidelberg: Springer Berlin Heidelberg, 2009, pp. 136–147.

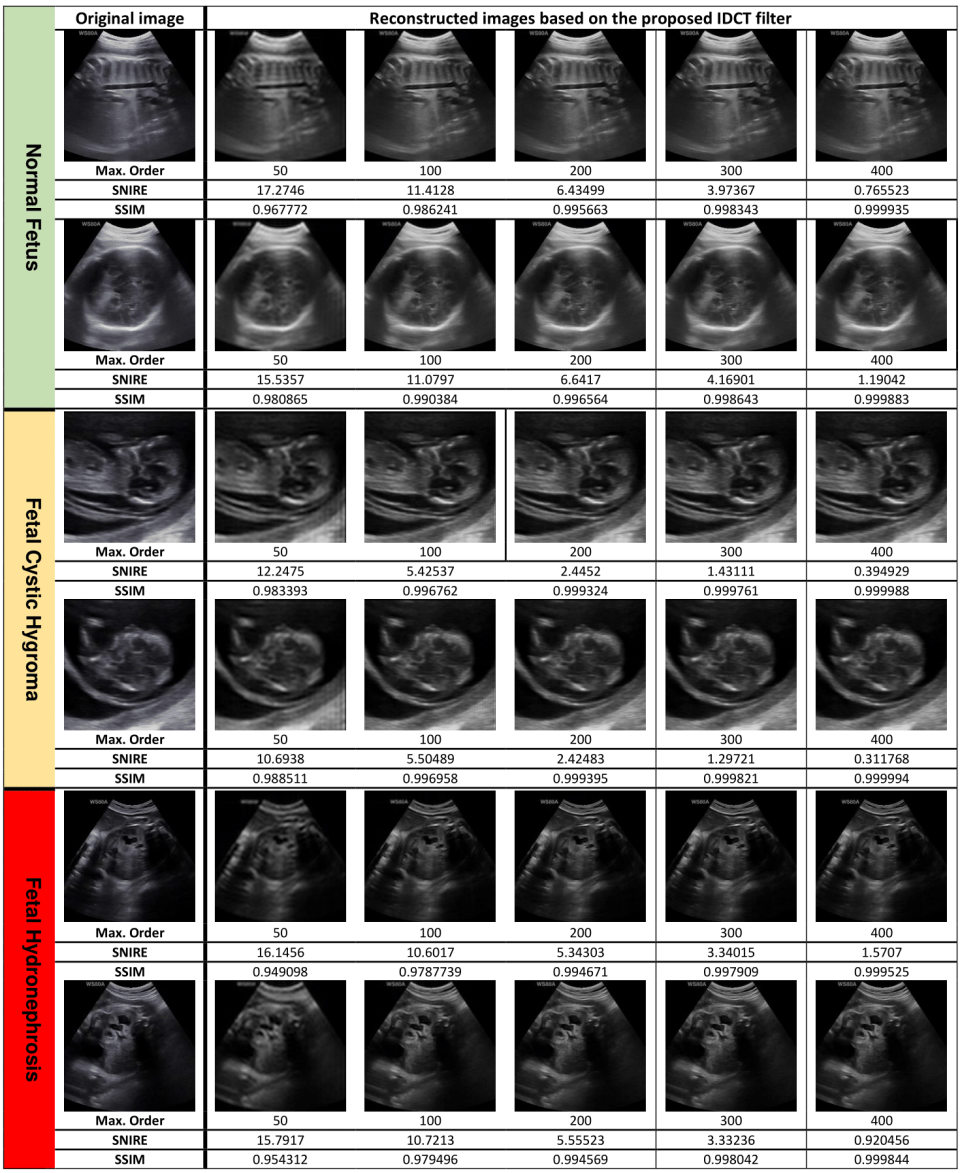

Fig. 8: Image reconstruction of ultrasound fetus images with different orders with their reconstruction errors using the proposed IDCT filter structure.

[7] A. Miri, S. Sharifian, S. Rashidi, and M. Ghods, "Medical image denoising based on 2d discrete cosine transform via ant colony optimization," *Optik*, vol. 156, pp. 938 – 948, 2018.

[8] V. V. L. Oleksiy B. Pogrebnyak, "Wiener discrete cosine transform-based image filtering," *Journal of Electronic Imaging*, vol. 21, no. 4, pp. 1 – 16 – 16, 2012.

[9] K. Chang, R. Paramesran, B. H. S. Asli, and C. Lim, "Efficient hardware accelerators for the computation of Tchebichef moments," *IEEE Transactions on Circuits and Systems for Video Technology*, vol. 22, no. 3, pp. 414–425, March 2012.

[10] B. H. S. Asli, R. Paramesran, and C.-L. Lim, "The fast recursive computation of Tchebichef moment and its inverse transform based on Z-transform," *Digital Signal Processing*, vol. 23, no. 5, pp. 1738–1746, 2013.

[11] S. Tsai and S.-M. Yang, "A fast DCT algorithm for watermarking in digital signal processor," *Mathematical Problems in Engineering*, vol. 2017, 2017.

[12] Nam Ik Cho and San Uk Lee, "Fast algorithm and implementation of 2-D discrete cosine transform," *IEEE Transactions on Circuits and Systems*, vol. 38, no. 3, pp. 297–305, 1991.

[13] G. Yu and G. Sapiro, "DCT Image Denoising: a Simple and Effective Image Denoising Algorithm," *Image Processing On Line*, vol. 1, pp. 292–296, 2011.

[14] S. S. Haykin, *Adaptive filter theory*. Pearson Education India, 2005.

[15] S. Gai, B. Zhang, C. Yang, and L. Yu, "Speckle noise reduction in medical ultrasound image using monogenic wavelet and laplace mixture distribution," *Digital Signal Processing*, vol. 72, pp. 192–207, 2018.

[16] R. Öktem, K. Egiazarian, V. V. Lukin, N. N. Ponomarenko, and O. V. Tsymbal, "Locally adaptive DCT filtering for signal-dependent noise removal," *EURASIP Journal on Advances in Signal Processing*, vol. 2007, no. 1, p. 042472, 2007.

[17] Y. Sheng and L. Shen, "Orthogonal Fourier–Mellin moments for invariant pattern recognition," *J. Opt. Soc. Am. A*, vol. 11, no. 6, pp. 1748–1757, Jun 1994.

[18] A. Mittal, A. K. Moorthy, and A. C. Bovik, "No-reference image quality assessment in the spatial domain," *IEEE Transactions on Image Processing*, vol. 21, no. 12, pp. 4695–4708, Dec 2012.

[19] A. Mittal, R. Soundararajan, and A. C. Bovik, "Making a "completely blind" image quality analyzer," *IEEE Signal Processing Letters*, vol. 20, no. 3, pp. 209–212, March 2013.

[20] D. Kundur and D. Hatzinakos, "Blind image deconvolution," *IEEE signal processing magazine*, vol. 13, no. 3, pp. 43–64, 1996.

Cranfield University

CERES https://dspace.lib.cranfield.ac.uk

School of Aerospace, Transport and Manufacturing (SATM) Staff publications (SATM)

2021-05-05

DCT/IDCT filter design for ultrasound image filtering

Shakibaei, Barmak Honarvar

IEEE

Shakibaei BH, Flusser J, Zhao Y, et al., (2021) DCT/IDCT filter design for ultrasound image filtering. In: IEEE 2020 25th International Conference on Pattern Recognition (ICPR 2020), 10-15 January 2021, Milan, Italy

https://doi.org/10.1109/ICPR48806.2021.9412838

Downloaded from Cranfield Library Services E-Repository